J|A|C|S
ARTICLES
Published on Web 10/12/2004

Pentadienyls vs Cyclopentadienyls and Reversal of Metal−Ligand Bonding Affinity with Metal Oxidation State: Synthesis, Molecular Structures, and Electronic Structures of High-Valent Zirconium Pentadienyl Complexes

Asha Rajapakshe,[1] Nadine E. Gruhn,[1] Dennis L. Lichtenberger,*[,1] Rehan Basta,[2] Atta M. Arif,[2] and Richard D. Ernst*[,2]

Contribution from the Center for Gas-Phase Electron Spectroscopy, Department of Chemistry, The University of Arizona, Tucson, Arizona 85721, and Department of Chemistry, The University of Utah, Salt Lake City, Utah 84112

Received May 3, 2004; E-mail: dlichten@email-arizona.edu; ernst@chem.utah.edu

Abstract: Molecules of the form Cp(6,6-dmch)ZrX_2 (Cp = η^5-cyclopentadienyl, X = Cl, Br, I; 6,6-dmch = η^5-6,6-dimethylcyclohexadienyl) have been synthesized, and the molecular and electronic structures have been investigated. These molecules allow direct comparison of the bonding and properties of pentadienyl and cyclopentadienyl ligands in the same high-oxidation-state metal complexes. Unlike the well-known Cp_2ZrX_2 analogues, these Cp(6,6-dmch)ZrX_2 molecules are intensely colored, indicating significantly different relative energies of the frontier orbitals. Also unusual, the average Zr−C distances to the 6,6-dmch pentadienyl ligand are about 0.1 Å longer than the average Zr−C distances to the cyclopentadienyl ligand for these Zr(IV) complexes, opposite of what is observed for the Zr(II) complex Cp(2,6,6-tmch)$Zr(PMe_3)_2$ (tmch = η^5-2,6,6-trimethylcyclohexadienyl), reflecting a dramatic reversal in the favorability of the bonding depending on the metal oxidation state. The experimental and computational results indicate that the color of the Cp(6,6-dmch)ZrX_2 complexes is due to a 6,6-dmch ligand-to-metal charge-transfer band. Compared to the Cp_2ZrX_2 analogues, the Cp(6,6-dmch)ZrX_2 molecules have a considerably less stable HOMO that is pentadienyl-based and an essentially unchanged metal-based LUMO. Also, the lowest unoccupied orbital of pentadienyl is stabilized relative to cyclopentadienyl and becomes a better potential delta electron acceptor, thus contributing to the differences in structure and reactivity of the low-valent and high-valent metal complexes.

Introduction

Pentadienyl ligands have been found to possess many unique and potentially useful properties, such as the ability to adopt a wide range of η^1, η^3, and η^5 bonding modes, an extreme tendency to bond to transition metals in low oxidation states as a result of these ligands' high δ acidities, and their quite substantial steric demands (greater than $C_5Me_5^-$), which contribute to the formation of a large number of stable, electron-deficient complexes. Additionally, it has been shown that pentadienyl ligands may be more strongly bound than the "stabilizing" cyclopentadienyl ($C_5H_5^-$) ligand, while simultaneously possessing higher reactivities.[3] The high reactivity of the electronically open pentadienyl ligands has led to a wide variety of interesting and useful reactions and applications, including coupling reactions,[4−6] "naked" metal chemistry,[7−9] metal and metal oxide film depositions,[10−12] materials syntheses,[13,14] polymerizations,[15] and the incorporation of metals into semiconductors.[16−18]

While many studies have contributed to the development of our understanding of the above aspects of metal-pentadienyl chemistry, due to the extreme favorability of low metal oxidation states ($\leq +2$) in these species, it must be recognized that a large

(1) The University of Arizona.
(2) The University of Utah.
(3) Ernst, R. D. *Comments Inorg. Chem.* **1999**, *21*, 285−325.
(4) Kralik, M.; Hutchinson, J.; Ernst, R. *J. Am. Chem. Soc.* **1985**, *107*, 8296−8297.
(5) Kulsomphob, V.; Harvey, B.; Arif, A. M.; Ernst, R. D. *Inorg. Chim. Acta* **2002**, *334*, 17−24, and references therein.
(6) Basta, R.; Arif, A. M.; Ernst, R. D. *Organometallics* **2003**, *22*, 812−817.
(7) Severson, S. J.; Cymbaluk, T. H.; Ernst, R.; Higashi, J. M.; Parry, R. *Inorg. Chem.* **1983**, *22*, 3833−3834.
(8) Elschenbroich, C.; Nowotny, M.; Behrendt, A.; Harms, K.; Wacadlo, S.; Pebler, J. *J. Am. Chem. Soc.* **1994**, *116*, 6217−6219.
(9) Newbound, T. D.; Freeman, J. W.; Wilson, D. R.; Kralik, M. S.; Patton, A. T.; Campana, C. F.; Ernst, R. D. *Organometallics* **1987**, *6*, 2432−2437.
(10) Spencer, J. T.; Ernst, R. D. U.S. Patent, 5,352,488, 1994.
(11) Meda, L. J.; Breitkopf, R.; Haas, T.; Kirss, R. U. *Proc. Mater. Res. Soc.* **1998**, *495*, 75.
(12) Meda, L. J.; Breitkopf, R.; Haas, T.; Kirss, R. U. *Proc. Mater. Res. Soc* **1998**, *495*, 51.
(13) Hessen, B.; Siegrist, T.; Palstra, T.; Tanzler, S. M.; Steigerwald, M. L. *Inorg. Chem.* **1993**, *32*, 5165−5169.
(14) Hessen, B.; Stuczynski, S. M.; Steigerwald, M. L. 205th National ACS Meeting; Denver, CO, March 28, 1993.
(15) Köhler, F. H.; Mölle, R.; Strauss, W.; Weber, B.; Gedridge, R. W.; Basta, R.; Trakarnpruk, W.; Tomaszewski, R.; Arif, A. M.; Ernst, R. D. *Organometallics* **2003**, *22*, 1923−30, and ref 7 therein.
(16) Dadgar, A.; Stenzel, O.; Kohne, L.; Naser, A.; Strassburg, M.; Stolz, W.; Bimberg, D.; Schumann, H. *J. Cryst. Growth* **1998**, *195*, 69−73.
(17) Dadgar, A.; Stenzel, O.; Naser, A.; Iqbal, M. Z.; Bimberg, D.; Schumann, H. *Appl. Phys. Lett.* **1998**, *73*, 3878−3880.
(18) Dadgar, A.; Bimberg, D.; Stenzel, O.; Schumann, H. German Patent, 19747996, 1999.

piece of the puzzle remains unaddressed. Given that cyclopentadienyl ligands can form stable complexes with at least heptavalent metals,[19] and considering the enormous fundamental and practical impacts of $(\eta^5\text{-}C_5H_5)_2MX_2$ complexes,[20−22] gaining an understanding of the fundamental properties, reactivities, and applications of η^5-pentadienyl ligands in higher ($\geq +3$) oxidation state complexes can be considered to be an important goal; in fact, this has been identified as the greatest remaining challenge in this field.[3] Clearly, the isolation of such species is a necessary prerequisite to any realistic attempts to gain an understanding of their nature.

Recent results have indicated that zirconium is capable of providing stable tetravalent η^5-pentadienyl complexes,[5,6,23,24] and herein are provided synthetic, spectroscopic, and structural data for the first general series of higher valent metal pentadienyl complexes, Cp(6,6-dmch)ZrX_2 (Cp = η^5-C_5H_5; X = Cl, Br, I; 6,6-dmch = 6,6-dimethylcyclohexadienyl). The 6,6-dmch ligand, whose use has been pioneered by Wolczanski,[25−27] displays the key pentadienyl features such as a high delta acidity and a favorability for bonding to metals in lower oxidation states, but, at least in conjunction with the electropositive metal zirconium, can lead to stable M(IV) species.

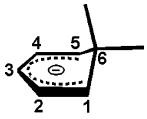

6,6-dmch

The intense deep orange to red colors of these Cp(6,6-dmch)ZrX_2 complexes, and of their (6,6-dmch)$_2ZrX_2$ analogues,[28] as opposed to the white or pale Cp_2ZrX_2 complexes reveal some dramatic differences between the open and closed dienyl ligands. Theoretical and bonding studies of the Cp(6,6-dmch)ZrX_2 series provide the heretofore missing insight into the major differences between the two ligand types for higher valent metal complexes. These species will now also allow for the investigation of the chemistry and applications of higher oxidation state pentadienyl analogues of the ubiquitous Cp_2MX_2 types of complexes.

This study will begin to address the above questions through an examination of the structures, valence ionizations, and orbital characters of Cp(6,6-dmch)ZrX_2 complexes for X = Cl, Br, and I. The photoelectron spectra will be compared to previous studies of the analogous Cp_2ZrX_2 complexes[29−31] in order to obtain a measure of the differences in the valence ionization energies and characters. The spectra show that the key difference occurs in the highest occupied molecular orbital (HOMO) in the 6,6-dmch complexes, which is predominantly pentadienyl in character and which causes these molecules to ionize at significantly lower energies than the corresponding molecules without a pentadienyl ligand. Theoretical calculations of the electronic structures agree with this observation and, furthermore, show that the lowest unoccupied molecular orbital (LUMO) of these molecules is metal based and changes very little in energy or character between the pentadienyl and Cp analogues. Calculations of the electronic excitations of these molecules by time-dependent density functional theory show that the colors of the 6,6-dmch molecules are due to the low-energy pentadienyl-to-metal (HOMO-to-LUMO) excitation. The same factors responsible for the low ionization energy of the highest occupied pentadienyl-based orbital also account for a low-lying unoccupied pentadienyl orbital that can act as an electron acceptor from the metal. The resulting "δ-acid" nature of the pentadienyl ligands contributes to the structural and reactivity differences found between the low-valent and high-valent metal complexes.

Experimental Section

Syntheses and Characterization of Compounds. All reactions were carried out under a nitrogen atmosphere in Schlenk apparatus, and the compounds were handled in a glovebox. Hydrocarbon solvents were dried by distillation from sodium benzophenone ketyl under nitrogen or with activated alumina under a nitrogen atmosphere. Cp(6,6-dmch)-$Zr(PMe_3)_2$ was prepared as previously described.[5] Cp_2ZrX_2 (X = Br and I) were synthesized according to published procedures.[32] NMR spectra were obtained as previously described,[33] and numbers of carbon atoms for the ^{13}C NMR data are included in accord with their assignments, but were not precisely integrated. Except for the parent ion (listed in italics), mass spectral peaks are listed only for those with relative abundances of at least 10%. Analytical data were obtained from Desert Analytics. UV/vis spectra were taken on a modified Cary 14 with OLIS interface (200−700 nm).

Dichloro(η^5-cyclopentadienyl)(η^5-6,6-dimethylcyclohexadienyl)-zirconium, Cp(6,6-dmch)$ZrCl_2$. To a dark black-red solution of Cp-(6,6-dmch)$Zr(PMe_3)_2$ (0.75 g, 1.8 mmol) in 30 mL of hexane under N_2 at 0 °C was added 1,2-dichloroethane (0.29 mL, 3.6 mmol). An orange precipitate immediately formed. The reaction mixture was allowed to stir for 1 h at room temperature. Next, it was filtered through a coarse frit and the solid was washed three times with ca. 40 mL of pentane, affording 0.25 g of orange powder (36% yield). The product was recrystallized from ca. 3 mL of toluene cooled to −30 °C.

^{1}H NMR (benzene-d_6, ambient): δ 0.58 (s, 3H, exo CH_3), 1.35 (s, 3H, endo CH_3), 4.44 (dd, 2H, J = 7.8, 1.5 Hz, $H_{1,5}$), 5.05 (tt, 1H, J = 5.7, 1.7 Hz, H_3), 5.82 (m, 2H, $H_{2,4}$), 5.98 (s, 5H, Cp). ^{13}C NMR (benzene-d_6, ambient): δ 28.07 (q, 1C, J = 125.7 Hz, exo CH_3), 31.56 (s, 1C, C_6), 34.29 (q, 1C, J = 126.7 Hz, endo CH_3), 95.04 (dt, 1C, J = 172.7, 7.7 Hz, C_3), 108.13 (d, 2C, J = 168.2 Hz, $C_{1,5}$), 115.99 (d of quintets, 5C, J = 175.3, 6.7 Hz, Cp), 125.67 (dd, 2C, J = 161.9, 7.8 Hz, $C_{2,4}$). UV/vis (hexane): lowest energy absorption, 440 nm (molar absorptivity, 3964 cm^{-1} M^{-1}), cf. Cp_2ZrCl_2 (acetonitrile), 343 nm (molar absorptivity, 793 cm^{-1} M^{-1}). Anal. Calcd for $C_{13}H_{16}Cl_2Zr$: C, 46.70; H, 4.82. Found: C, 46.85; H, 4.78.

Dibromo(η^5-cyclopentadienyl)(η^5-6,6-dimethylcyclohexadienyl)-zirconium, Cp(6,6-dmch)$ZrBr_2$. To a dark red solution of Cp(6,6-

(19) Herrmann, W. A. *Angew. Chem., Int. Ed. Engl.* **1988**, *27*, 1297−1313.
(20) Togni, A., Halterman, R., Eds. *Metallocenes: Synthesis, Reactivity, Applications*; Wiley-VCH: Weinheim, New York, 1998.
(21) Cardin, D. J.; Lappert, M. F.; Raston, C. *Chemistry Of Organo-Zirconium and Hafnium Compounds*; Halsted Press: New York, 1986.
(22) Marek, I., Ed. *Titanium and Zirconium in Organic Synthesis*; Wiley-VCH: Weinheim, Cambridge, England, 2002.
(23) Pillet, S.; Wu, G.; Kulsomphob, V.; Harvey, B. G.; Ernst, R. D.; Coppens, P. *J. Am. Chem. Soc.* **2003**, *125*, 1937−1949.
(24) Kulsomphob, V.; Arif, A. M.; Ernst, R. D. *Organometallics* **2002**, *21*, 3182−3188.
(25) DiMauro, P. T.; Wolczanski, P. T. *Organometallics* **1987**, *6*, 1947−1954.
(26) DiMauro, P.; Wolczanski, P.; Parkanyi, L.; Petach, H. *Organometallics* **1990**, *9*, 1097−1106.
(27) DiMauro, P. T.; Wolczanski, P. T. *Polyhedron* **1995**, *14*, 149−165.
(28) Basta, R.; Arif, A. M.; Ernst, R. Unpublished results.
(29) Petersen, J. L.; Lichtenberger, D. L.; Fenske, R. F.; Dahl, L. F. *J. Am. Chem. Soc.* **1975**, *97*, 6433−6450.
(30) Condorelli, G.; Fragalá, I.; Centineoe, A.; Tondello. *J. Organomet. Chem.* **1975**, *87*, 311−315.
(31) Cauletti, C.; Clark, J. P.; Green, J. C.; Jackson, S. E.; Fragalá, I. L.; Ciliberto, E.; Coleman, A. W. *J. Electron Spectrosc. Relat. Phenom.* **1980**, *18*, 61−73.
(32) Druce, P. M.; Kingston, B. M.; Lappert, M. F.; Spalding, T. R.; Srivastava, R. C. *J. Chem. Soc. (A)* **1969**, 2106−2110.
(33) Newbound, T. D.; Stahl, L.; Ziegler, M. L.; Ernst, R. D. *Organometallics* **1990**, *9*, 2962−2972.

dmch)Zr(PMe_3)$_2$ (0.50 g, 1.2 mmol) in 30 mL of hexane under N_2 at 0 °C was added 1,2-dibromoethane (0.16 mL, 1.8 mmol). A red-orange precipitate immediately formed. The reaction mixture was allowed to stir for 1 h. The solvent was removed in vacuo, leaving a red-orange residue. The product was extracted with ca. 40 mL of toluene. The solution was filtered through a Celite pad on a coarse frit. The product was recrystallized by concentration of the filtrate in vacuo to ca. 4 mL and cooling to −30 °C, which afforded 0.24 g (47% yield) of red-orange crystals.

^{1}H NMR (benzene-d_6, ambient): δ 0.56 (s, 3H, exo CH_3), 1.27 (s, 3H, endo CH_3), 4.54 (dd, 2H, J = 7.9, 1.4 Hz, $H_{1,5}$), 5.24 (tt, 1H, J = 5.8, 1.7 Hz, H_3), 5.85 (m, 2H, $H_{2,4}$), 6.01 (s, 5H, Cp). ^{13}C NMR (benzene-d_6, ambient): δ 29.01 (q, 1C, J = 126.2 Hz, exo CH_3), 31.88 (s, 1C, C_6), 34.28 (q, 1C, J = 131.4 Hz, endo CH_3), 97.30 (dt, 1C, J = 173.5, 7.7 Hz, C_3), 108.16 (d, 2C, J = 163.4 Hz, $C_{1,5}$), 115.99 (d of quintets, 5C, J = 175.8, 6.7 Hz, Cp), 124.83 (dd, 2C, J = 161.3, 7.0 Hz, $C_{2,4}$). UV/vis (hexane): lowest energy absorption, 464 nm (molar absorptivity, 4976 cm^{-1} M^{-1}), cf. Cp_2ZrBr_2 (acetonitrile), 375 nm (molar absorptivity, 1387 cm^{-1} M^{-1}). Anal. Calcd for $C_{13}H_{16}Br_2Zr$: C, 36.90; H, 3.81. Found: C, 37.15; H, 3.73.

Diiodo(η^5-cyclopentadienyl)(η^5-6,6-dimethylcyclohexadienyl)zirconium, Cp(6,6-dmch)ZrI$_2$. To a dark black-red solution of Cp(6,6-dmch)Zr(PMe_3)$_2$ (0.98 g, 2.36 mmol) in 30 mL of hexane under N_2 at room temperature was added 1,2-diiodoethane (0.70 g, 2.36 mmol). A bright red precipitate immediately formed. The reaction mixture was allowed to stir for 1 h. Next, it was filtered through a coarse frit and the red solid was washed using ca. 40 mL of pentane, affording 1.08 g (88% yield) of crude product as a red powder. The product was recrystallized from ca. 15 mL of toluene at −30 °C, yielding 0.37 g (30% yield).

^{1}H NMR (benzene-d_6, ambient): δ 0.54 (s, 3H, exo CH_3), 1.12 (s, 3H, endo CH_3), 4.71 (dd, 2H, J = 7.8, 1.5 Hz, $H_{1,5}$), 5.61 (tt, 1H, J = 5.8, 1.5 Hz, H_3), 5.84 (m, 2H, $H_{2,4}$) 6.06 (s, 5H, Cp). ^{13}C NMR (benzene-d_6, ambient): δ 30.33 (q, 1C, J = 126.2 Hz, exo CH_3), 32.06 (s, 1C, C_6), 34.37 (q, 1C, J = 127.1 Hz, endo CH_3), 99.41 (dt, 1C, J = 175.8, 8.1 Hz, C_3), 107.08 (d, 2C, J = 163.9 Hz, $C_{1,5}$), 115.16 (d of quintets, 5C, J = 176.5, 6.7 Hz, Cp), 122.85 (dd, 4C, J = 164.0, 7.9 Hz, $C_{2,4,10,12}$). MS (EI, 23 eV) *m/z* (relative intensity): 91 (19), 93 (39), 107 (19), 317 (10), 409 (100), 410 (24), 411 (34), 413 (32), 501 (85), 502 (28), 503 (28), 505 (27), *516(6)*. UV/vis (hexane): lowest energy absorption, 489 nm (molar absorptivity, 4081 cm^{-1} M^{-1}), cf. Cp_2ZrI_2 (acetonitrile), 408 nm (molar absorptivity, 848 cm^{-1} M^{-1}). Anal. Calcd for $C_{13}H_{16}I_2Zr$: C, 30.19; H, 3.12. Found: C, 30.36; H, 3.13.

X-ray Diffraction Studies. Single crystals of the compounds were grown from toluene solutions as described above. The crystals were fixed to glass fibers using Paratone oil and transferred to a Nonius Kappa CCD diffractometer. Data pertaining to the structural study are provided in Table 1. Structures were solved with direct methods, and all non-hydrogen atoms were refined anisotropically. The hydrogen atoms in one methyl group of the dichloride complex were placed in idealized locations, while all other hydrogen atoms were refined isotropically. All computations utilized the SHELX97 programs (G. Sheldrick, University of Göttingen).

Photoelectron Data Collection. Photoelectron spectra were recorded using an instrument that features a 36 cm hemispherical analyzer[34] and custom-designed photon source, sample cells, and detection and control electronics.[35] The excitation source is a quartz capillary discharge lamp with the ability, depending on operating conditions, to produce He I (21.218 eV) or He II (40.814 eV) photons. The ionization energy scale was calibrated using the $^2P_{3/2}$ ionization of argon (15.759 eV) and the $^2E_{1/2}$ ionization of methyl iodide (9.538 eV). The argon $^2P_{3/2}$ ionization also was used as an internal calibration lock of the absolute ionization energy to control spectrometer drift throughout data collection. During He I and He II data collection the instrument resolution, measured using the full-width-at-half-maximum of the argon $^2P_{3/2}$ ionization, was 0.024−0.030 eV. All of the spectra were corrected for the presence of ionizations caused by other emission lines from the discharge source.[36] The He I spectra were corrected for the He Iβ line (1.866 eV higher in energy and 3% the intensity of the He Iα line), and the He II spectra were corrected for the He IIβ line (7.568 eV higher in energy and 12% the intensity of the He IIα line). All data also were intensity corrected with an experimentally determined instrument analyzer sensitivity function that assumes a linear dependence of analyzer transmission (intensity) to the kinetic energy of the electrons within the energy range of these experiments. In the figures of the data, the vertical length of each data mark represents the experimental variance of that point.[37]

Table 1. Crystal Data and Refinement Parameters for the Zr(C_5H_5)(6,6-dmch)X_2 Complexes

	Cl	Br	I
formula	$C_{13}H_{16}Cl_2$ Zr	$C_{13}H_{16}Br_2$ Zr	$C_{13}H_{16}I_2$ Zr
fw	334.38	423.30	517.28
temperature, K	150(1)	150(1)	150(1)
λ, Å	0.71073	0.71073	0.71073
cryst syst	monoclinic	triclinic	monoclinic
space group	$P2_1/c$	$P\bar{1}$	$P2_1/n$
a, Å	17.5859(7)	6.8198(3)	8.7300(2)
b, Å	6.64510(10)	9.4658(7)	13.1929(3)
c, Å	24.7237(10)	11.7016(8)	13.0595(4)
α, deg	90.0	91.077(3)	90.0
β, deg	107.9458(12)	103.919(4)	95.2980(11)
γ, deg	90.0	104.246(4)	90.0
volume, Å^3; Z	2748.65(16); 8	708.22(8); 2	1497.69(7); 4
density (calc), g cm^{-3}	1.616	1.985	2.294
abs coeff, cm^{-1}	11.60	63.91	48.31
θ range, deg	4.2−27.5	3.4−27.5	3.3−27.5
limiting indices	$-22 \le h \le 22$ $-8 \le k \le 6$ $-32 \le l \le 31$	$-7 \le h \le 8$ $-10 \le k \le 12$ $-15 \le l \le 13$	$-11 \le h \le 11$ $-17 \le k \le 15$ $-16 \le l \le 16$
no. of reflns collected	5066	4897	6347
no. of indep reflns; n: $I > n\sigma(I)$	3119; 2	3181; 2	3412; 2
$R(F)$	0.0376	0.0573	0.0390
$R(wF^2)$	0.0684	0.1539	0.0871
max./min. diff Fourier peak, e/Å^3	0.46/−0.52	1.82/−1.73	1.18/−1.16

The samples sublimed cleanly with no visible changes in the spectra during data collection. The sublimation temperatures (in °C, at 10^{-4} Torr) were as follows: Cp(6,6-dmch)$ZrCl_2$, 80−110; Cp(6,6-dmch)-$ZrBr_2$, 88−116; Cp(6,6-dmch)ZrI_2, 94−150; Cp_2ZrCl_2, 90−150; Cp_2-$ZrBr_2$, 120−136; Cp_2ZrI_2, 90−130 (monitored using a "K" type thermocouple passed through a vacuum feedthrough and attached directly to the ionization cell).

Photoelectron Data Analysis. The valence ionization bands are represented analytically with the best fit of asymmetric Gaussian peaks, as described in more detail elsewhere.[37] The Gaussians are defined with the position, amplitude, half-width for the high binding energy side of the peak, and the half-width for the low binding energy side of the peak. The peak positions and half-widths are reproducible to about ±0.02 eV (≈3σ level). The parameters describing an individual ionization are less certain when two or more peaks are close in energy and are overlapping. If the combined band contour does not contain sufficient information for independent determination of the individual peak parameters, the number of peaks and/or independent parameters in the analytical representation are appropriately reduced. These situations are evident in the tables, where half-widths for similar peaks

(34) Siegbahn, K.; Nordling, C.; Fahlman, A.; Nordberg, R.; Hamrin, K.; Hedman, J.; Johansson, G.; Bergmark, T.; Karlsson, S.-E.; Lindgren, I.; Lindberg, B. *ESCA: Atomic, Molecular and Solid State Structure Studied by Means of Electron*; Almqvist & Wiksells: Uppsala, 1967.
(35) Lichtenberger, D. L.; Kellogg, G. E.; Kristofzski, J. G.; Page, D.; Turner, S.; Klinger, G.; Lorenzen. *J. Rev. Sci. Instrum.* **1986**, *57*, 2366.
(36) Turner, D. W.; Baker, C.; Baker, A. D.; Brundle, C. R. *Molecular Photoelectron Spectroscopy*; Wiley-Interscience: London, 1970.
(37) Lichtenberger, D. L.; Copenhaver, A. S. *J. Electron Spectrosc. Relat. Phenom.* **1990**, *50*, 335−352.

are occasionally constrained to be the same. When a region of broad ionization intensity spans numerous overlapping ionization bands, the individual parameters of the Gaussian peaks used to model the total ionization intensity are not characteristic of individual ionization states. To avoid misinterpretation, only the total analytical fit is displayed in these regions and the individual peak parameters are not listed in the tables or displayed in the figures.

Confidence limits for the relative integrated peak areas are about 5%, with the primary source of uncertainty being the determination of the baseline under the peaks. The baseline is caused by electron scattering and taken to be linear over the small energy range of these spectra. The total area under a series of overlapping peaks is known with the same confidence, but the individual peak areas are less certain.

Computational Methodology. Electronic structure calculations were carried out to compare the energies and characters of the orbitals with the results of the photoelectron experiments and to investigate the colors of the molecules. Initial geometries of the pentadienyl molecules were taken from the crystal structures and were optimized by density functional theory using the package ADF 2003.01.[38] These calculations were carried out at the GGA (generalized gradient approximation) level with BLYP (Becke exchange[39] and LYP correlation function[40]). The TZP (valence triple-ζ with a polarization function) Slater-type basis set was used. The orbital plots were generated using the program Molekel.[41] The first vertical ionization energies of all molecules were calculated as the difference between the total energy of the positive ion and the neutral molecule at the optimized neutral molecule geometry (ΔE_{SCF}).

Time-dependent density functional calculations (TD-DFT[42,43]) of the electronic excitations of Cp_2ZrX_2 and Cp(6,6-dmch)ZrX_2 were performed at the geometries obtained above but with GRACLB[44] (the gradient-regulated asymptotic correction, which in the outer region closely resembles the LB94[45]) potential as the XC functional. The dipole-allowed singlet excitation energies were studied using the TZP basis set. Further experiments on varying the error tolerance in the square of the excitation energies and the dependency revealed that the results are independent of those variables. A dependency check showed no numerical problems associated with the linear dependencies in the basis set.

Results

Syntheses and Characterization of the Cp(6,6-dmch)ZrX_2 Complexes. The Cp(6,6-dmch)ZrX_2 complexes were prepared from the reaction of Cp(6,6-dmch)Zr$(PMe_3)_2$ with dihaloalkanes. Initial attempts with C_2Cl_6, which has been found to be a useful chlorination reagent for other metal complexes,[46] led to rapid reactions and the formation of traces of reddish crystalline material, but large amounts of accompanying insoluble products, presumed to result from further chlorination by C_2Cl_4. To avoid this problem, and also to avoid the formation of explosive haloalkynes, resort was made to 1,2-dihaloalkanes. With these reagents, much larger quantities of products could be obtained (eq 1). These compounds have been characterized by standard analytical and spectroscopic methods (see Experimental Section).

$$\text{Cp(6,6-dmch)Zr}(PMe_3)_2 + \text{1,2-}C_2H_4X_2 \rightarrow \text{Cp(6,6-dmch)}ZrX_2\ X = \text{Cl, Br, I} \quad (1)$$

As opposed to their pale-colored Cp_2ZrX_2 analogues, these species are highly colored, varying from orange (X = Cl) to red-orange (X = Br) to red (X = I). Clearly there are substantial electronic differences in the M−Cp and M−pentadienyl electronic structures and bonding, which will be addressed later in this section. Substantial chemical differences also have been observed, especially the susceptibility of these complexes to loss of a 6,6-dmch ligand upon exposure to donor ligands, such as dmpe.[28] The results of these studies will be reported separately. The facile loss of a pentadienyl ligand is a typical reaction for a higher valent metal center, in accord with the extreme preference of these ligands for low-valent metal centers. Indeed, even similar attempts to chlorinate Ti$(6,6\text{-dmch})_2$ lead to polymeric Ti(6,6-dmch)Cl_2.[28]

One other class of related compounds is known, having a substituted boron center bridging the two ends of the dienyl ligand.[47−51] However, the boron bridges in these boratabenzene complexes have long been recognized to be noninnocent, especially in being positioned in the dienyl plane,[52,53] whereas a fold angle of ca. 40° is observed in cyclohexadienyl complexes such as these (38.2°, 39.0°, and 40.3°, respectively, for Cl, Br, and I). The boratabenzene complexes, therefore, are really η^6 arene ligands rather than η^5 dienyls.

The solid-state structures of the dihalide complexes were determined by X-ray diffraction, and the results are presented in Figure 1 and Tables 1 and 2. In each case, a bent sandwich arrangement is observed, similar to that of related metallocene dihalides. In the prototypical Cp_2ZrCl_2,[54,55] one observes a Cp(centroid)−Zr−Cp(centroid) angle of 129° and a Cl−Zr−Cl angle of 97° in comparison to the corresponding values of 126° and 96° for the Cp(6,6-dmch)$ZrCl_2$ complex. In each of the structures reported here, the two halides are positioned by one of the external dienyl C−C bonds (C4−C5), leading to a significant lengthening of these Zr−C bonds relative to their C1 and C2 counterparts. Even more notable, however, is the substantial lengthening in Zr−C bonds as one proceeds from C3 to the terminal carbon atoms (C1, C5). Some of the Zr−C5 distances are more than 0.3 Å longer than the Zr−C3 distances, seeming to reflect difficulties for the contracted Zr(IV) center in maintaining overlap with the entire dienyl ligand. This then provides a fairly clear depiction of the unfavorability of η^5 pentadienyl coordination for a high oxidation state metal center. Indeed, the distortion of the bonding in these cases likely presents a picture of an intermediate in the spontaneous

(38) Te Velde, G.; Bickelhaupt, F.; Baerends, E.; Fonseca Guerra, C. *J. Comput. Chem.* **2001**, *22*, 931−967.
(39) Becke, A. D. *Phys. Rev. A: At., Mol., Opt. Phys.* **1988**, *38*, 3098−3100.
(40) Lee, C.; Yang, W.; Parr, R. G. *Phys. Rev. B* **1988**, *37*, 785.
(41) Flukier, P.; Luthi, H. P.; Portmann, S.; Weber, J. *Molekel 4.1*; Swiss Center for Scientific Computing: Manno, Switzerland, 2000−2001.
(42) van Gisbergen, S. J. A.; Snijders, J. G.; Baerends, E. J. *Comput. Phys. Commun.* **1999**, *118*, 119−138.
(43) Gross, E. K. U., Dobson, J. F., Petersilka, Nalewajski, R. F., Eds. *Density Functional Theory*; Springer: Heidelberg, 1996.
(44) Gruning, M.; Gritsenko, O. V.; van Gisbergen, S. J. A.; Baerends, E. J. *J. Chem. Phys.* **2001**, *114*, 661−660.
(45) van Leeuwen, R.; Baerends, E. J. *Phys. Rev. A: At., Mol., Opt. Phys.* **1994**, *49*, 2421−2431.
(46) Deacon, G.; Feng, T.; Nickel, S.; Skelton, B.; White, A. *Chem. Commun.* **1993**, 1328.
(47) Bazan, G. C.; Cotter, W. D.; Komon, Z. J. A.; Lee, R. A.; Lachicotte, R. J. *J. Am. Chem. Soc.* **2000**, *122*, 1371−1380.
(48) Lee, B. Y.; Bazan, G. C. *J. Organomet. Chem.* **2002**, *642*, 275−279.
(49) Ashe, A. J., III; Al-Ahmad, S.; Fang, X.; Kampf, J. W. *Organometallics* **2001**, *20*, 468−473.
(50) Ashe, A. J., III; Kampf, J. W.; Schiesher, M. W. *Organometallics* **2003**, *22*, 203−206.
(51) Herberich, G. E.; Englert, U.; Ganter, B.; Pons, M. *Eur. J. Inorg. Chem.* **2000**, *2000*, 979−986.
(52) Herberich, G. E.; Greiss, G. *Chem. Ber.* **1972**, *105*, 3413−3423.
(53) Herberich, G. E.; Ohst, H. *Adv. Organomet. Chem.* **1986**, *25*, 199−236.
(54) Corey, J. Y.; Zhu, X.; Rath, L. B. A. P. *Acta Crystallogr.* **1995**, 565−657.
(55) Repo, T.; Klinga, M.; Mutikainen, I.; Su, Y.; Leskela, M.; Polamo, M. *Acta Chem. Scand.* **1996**, *50*, 1116−1120.

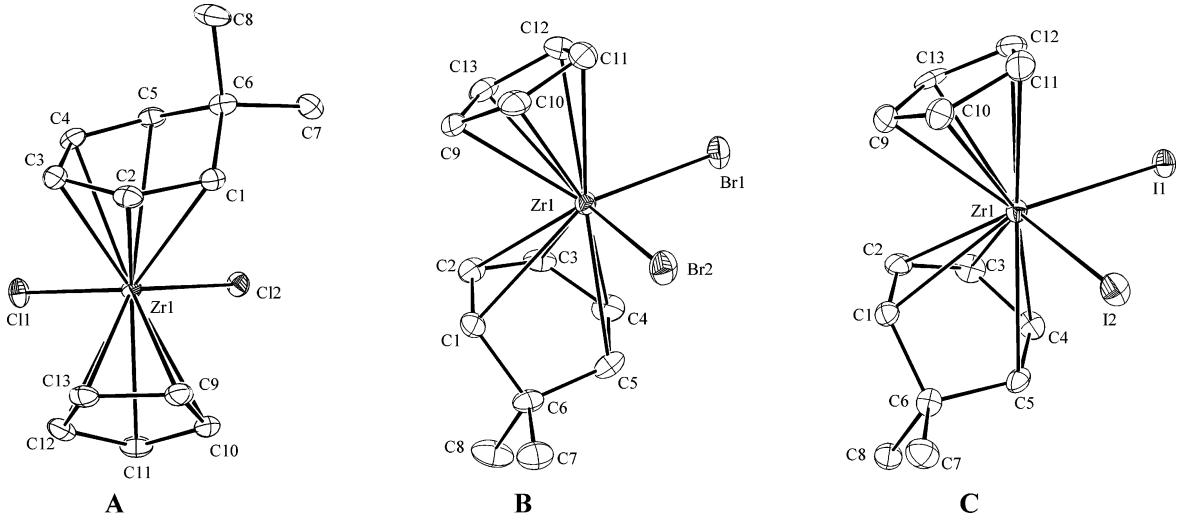

Figure 1. ORTEP diagrams of Cp(6,6-dmch)ZrX_2 complexes [(A) X = Cl, (B) X = Br, and (C) X= I] showing 50% thermal ellipsoids (hydrogens excluded).

Table 2. Comparison of Pertinent Experimental Structural Values [Calculated][a] for the $Zr(C_5H_5)$(6,6-dmch)X_2 Complexes

	X =		
	Cl	Br	I
	Distances (Å)		
Zr−X1	2.4649(9) [2.515]	2.6316(9)[2.704]	2.8673(5) [2.999]
Zr−X2	2.4463(8) [2.507]	2.6079(9) [2.689]	2.8491(5) [2.958]
Zr−C1	2.620(5) [2.801]	2.657(7) [2.812]	2.579(5) [2.729]
Zr−C2	2.519(4) [2.631]	2.518(7) [2.635]	2.502(5) [2.610]
Zr−C3	2.472(5) [2.571]	2.458(7) [2.567]	2.464(5) [2.582]
Zr−C4	2.570(4) [2.692]	2.577(7) [2.690]	2.563(5) [2.692]
Zr−C5	2.786(3) [2.936]	2.786(7) [2.943]	2.753(6) [2.919]
Zr−C (dmch[b], av)	2.593 [2.726]	2.599 [2.729]	2.572 [2.706]
Zr−C (Cp, av)	2.501(3) [2.620]	2.505(7) [2.619]	2.502(8) [2.612]
Zr−Cp plane	2.199 [2.322]	2.199 [2.321]	2.201 [2.312]
Zr−dmch[b] plane	2.210 [2.355]	2.213 [2.359]	2.191 [2.332]
	Angles (deg)		
X−Zr−X	95.95(4), 97.13(5) [99.97]	96.95(3) [99.29]	95.05(2) [98.06]
dmch−Zr−Cp	54.0, 55.0 [50.74]	54.5 [51.22]	54.7 [49.84]

[a] The structural values for CpZr(6,6-dmch)X_2 calculated from ADF. [b] C_1 to C_5 atoms of 6,6-dmch.

reduction process which takes place on the general attempted preparations of higher valent metal pentadienyl complexes, resulting in the expulsion of the pentadienyl fragment.[3] As noted above, the addition of a strongly binding ligand such as dmpe (1,2-(dimethylphosphino)ethane) can complete the dienyl expulsion process.

Of most interest, however, is the comparison of the relative bonding of the two dienyl ligand types. The Zr−C(pentadienyl) distances for these Zr(IV) complexes are on average ca. 0.1 Å longer than the Zr−C(Cp) distances in the same molecules (Table 2). The opposite trend is observed for Zr(II) molecules.[23,24] This rather drastic reversal of bonding favorability provides a dramatic confirmation of the long recognized preference of the electronically open dienyl ligands for metals in lower oxidation states. This issue will be discussed in greater detail after consideration of the electronic structures of the complexes.

Photoelectron Spectra. The He I photoelectron spectra for Cp(6,6-dmch)$ZrCl_2$, Cp(6,6-dmch)$ZrBr_2$, and Cp(6,6-dmch)ZrI_2 in the region from 7 to 12 eV are shown in Figure 2. The spectra are modeled analytically with asymmetric Gaussian peaks for quantitative comparison of the ionizations (Table 3), but the ionization features that provide the information and comparisons on these molecules are visually apparent in the spectra without this data analysis. On the basis of previous photoelectron studies of related cyclopentadienyl and pentadienyl metal halides, the ionizations expected in this region derive from the first two π ionizations of the 6,6-dmch ligand, the first two π ionizations of Cp, four pπ ionizations of the halogens, and two Zr−halogen σ bond ionizations.[29−31,56,57] Valence ionizations at higher energy are from the C−C and C−H σ bonds and the most stable π bond orbitals of 6,6-dmch and Cp. A description of the ionizations of each molecule is followed by a discussion of the trends in ionization energies.

CpZr(6,6-dmch)Cl_2. The assignment of the Cp(6,6-dmch)-$ZrCl_2$ spectrum is aided by the photoelectron spectrum of Cp_2-$ZrCl_2$, which is well understood from previous work.[29−31,58] The valence ionizations of these two molecules are compared in Figure 3. The first three bands in the low ionization energy

(56) Boehm, M. C.; Eckert-Maksic, M.; Ernst, R. D.; Wilson, D. R.; Gleiter, R. *J. Am. Chem. Soc.* **1982**, *104*, 2699−2707.
(57) Gleiter, R.; Hyla-Kryspin, I.; Ziegler, M. L.; Sergeson, G.; Green, J. C.; Stahl, L.; Ernst, R. D. *Organometallics* **1989**, *8*, 294−306.
(58) Fragalá, I.; Marks, T. J.; Fagan, P. J.; Manriquez, J. M. *J. Electron Spectrosc. Relat. Phenom.* **1980**, *20*, 253−258.

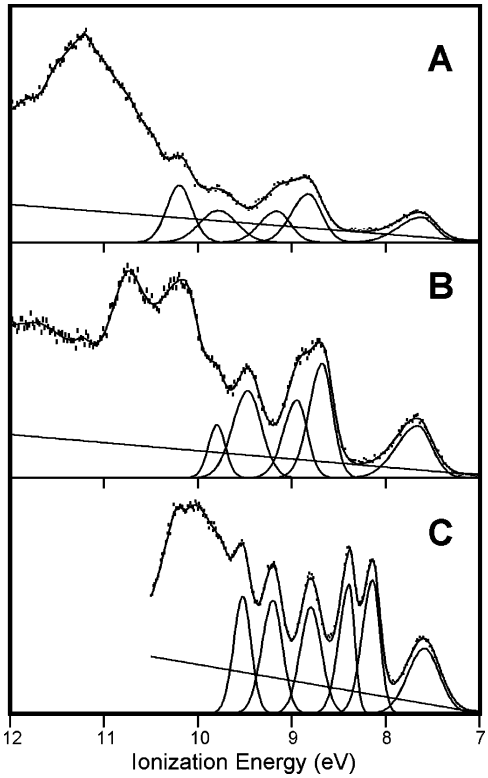

Figure 2. Valence photoelectron spectra of (A) Cp(6,6-dmch)$ZrCl_2$, (B) Cp(6,6-dmch)$ZrBr_2$, and (C) Cp(6,6-dmch)ZrI_2.

Table 3. Fit Parameters[a] and General Assignments and Labels of Ionizations

position	half-width high, low	relative area[b] He I	relative area[b] He II/He I	label
	Cp(6,6-dmch)$ZrCl_2$			
7.63	0.56, 0.36	1	1	dmch1
8.83	0.42, 0.34	1.59	0.66	Cp1
9.16	0.42, 0.34	1.02	0.55	Cp2
9.78	0.46, 0.46	1.27	0.48	dmch2
10.20−12.00				C1
	Cp(6,6-dmch)$ZrBr_2$			
7.66	0.53, 0.36	1	1	dmch1
8.68	0.34, 0.26	1.48	0.55	Cp1
8.95	0.34, 0.26	1.00	0.54	Cp2
9.47	0.38, 0.35	1.37	0.37	dmch2
9.80−11.00				Br
	Cp(6,6-dmch)ZrI_2			
7.59	0.41, 0.38	1	1	dmch1
8.14	0.27, 0.19	1.18	0.61	I(1)
8.39	0.26, 0.14	1.00	0.62	I(2)
8.80	0.27, 0.27	1.11	0.84	I(3)
9.20	0.28, 0.24	1.15	0.99	I(4)
9.52	0.23, 0.21	1.40	1.39	dmch2

[a] All energies in eV. [b] Relative to peak assigned area = 1.

region of the spectrum of Cp_2ZrCl_2 from about 8.5 to 10 eV are predominantly Cp(π) ionizations, while the ionizations from about 10 to 12 eV relate to molecular orbitals of primarily Cl 3p nature. The most striking difference between the ionizations of Cp_2ZrCl_2 and the ionizations of Cp(6,6-dmch)$ZrCl_2$ is the first ionization band at 7.60 eV in the spectrum of Cp(6,6-dmch)$ZrCl_2$. This ionization is much lower in energy than the first ionization of Cp_2ZrCl_2 and must correspond to ionization from a molecular orbital with dominant 6,6-dmch π character. The next two ionizations at 8.79 and 9.12 eV can be assigned as predominantly cyclopentadienyl π ionizations on the basis

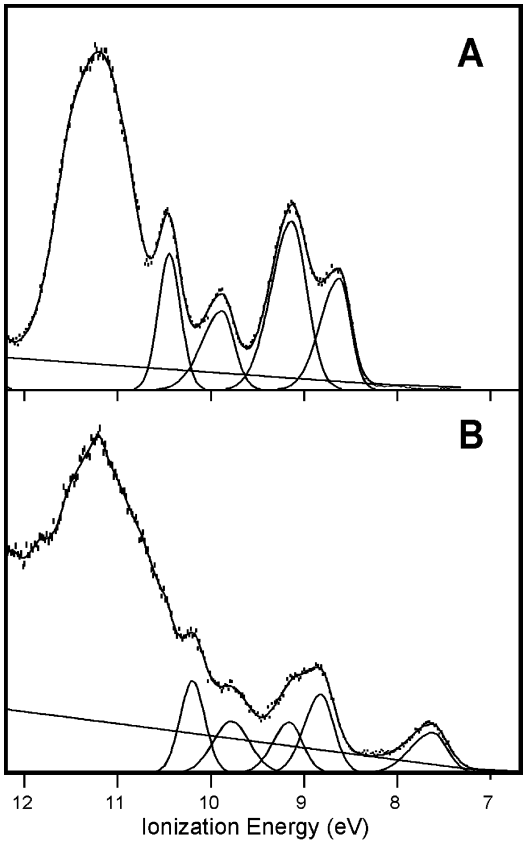

Figure 3. He I photoelectron spectra of (A) Cp_2ZrCl_2 and (B) Cp(6,6-dmch)$ZrCl_2$.

Table 4. Theoretical Atomic Photoionization Cross Sections per Valence Electron[83]

atom (orbital)	photoionization cross section (Mbarn) He I	photoionization cross section (Mbarn) He II	He II/He I ratio in relation to C
Zr (4d)	12.19	1.74	0.46
C (2p)	6.12	1.89	1
Cl (3p)	13.88	0.64	0.15
Br (4p)	15.57	0.97	0.20
I (5p)	7.99	0.78	0.32

of comparison with the spectrum of Cp_2ZrCl_2. However, as will be shown below, these Cp orbitals are mixed with some halide character and may also contain some 6,6-dmch character. The ionization intensity around 12 eV in the spectrum of Cp(6,6-dmch)$ZrCl_2$ that is not seen in the spectrum of Cp_2ZrCl_2 is due to the initial C−H σ ionizations of the methyl groups of Cp-(6,6-dmch)$ZrCl_2$.

He II spectra are useful to gain insight into the atomic character associated with each ionization band.[59] As seen in Table 4, ionizations arising from primarily halogen-based orbitals are expected to decrease in relative intensity compared to the ionizations arising from carbon-based orbitals when the photon source is switched from He I to He II.

The He I and He II close-up spectra of Cp(6,6-dmch)$ZrCl_2$ are compared in Figure 4. The intensity of ionization bands in the region above 10 eV decreases relative to the bands below 10 eV, supporting the assignment of the bands above 10 eV to ionizations containing more chlorine character. The ionization

(59) Green, J. C. *Acc. Chem. Res.* **1994**, *27*, 131−137.

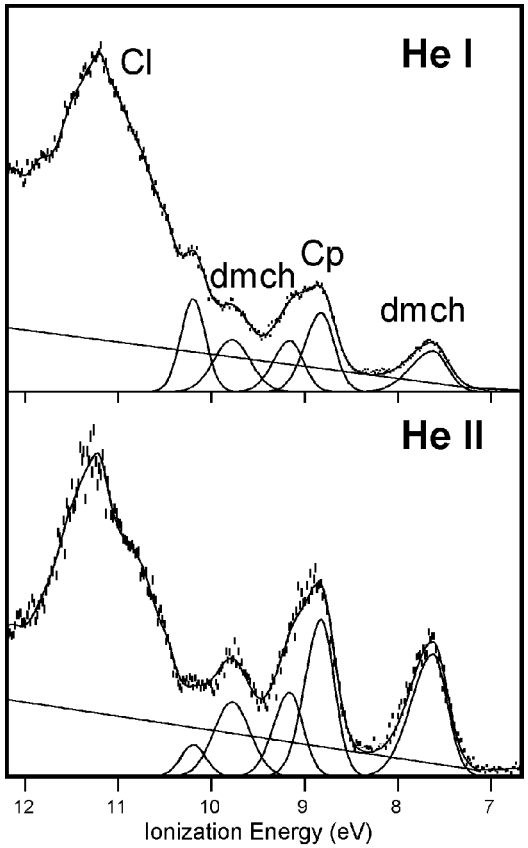

Figure 4. He I and He II photoelectron spectra of Cp(6,6-dmch)$ZrCl_2$.

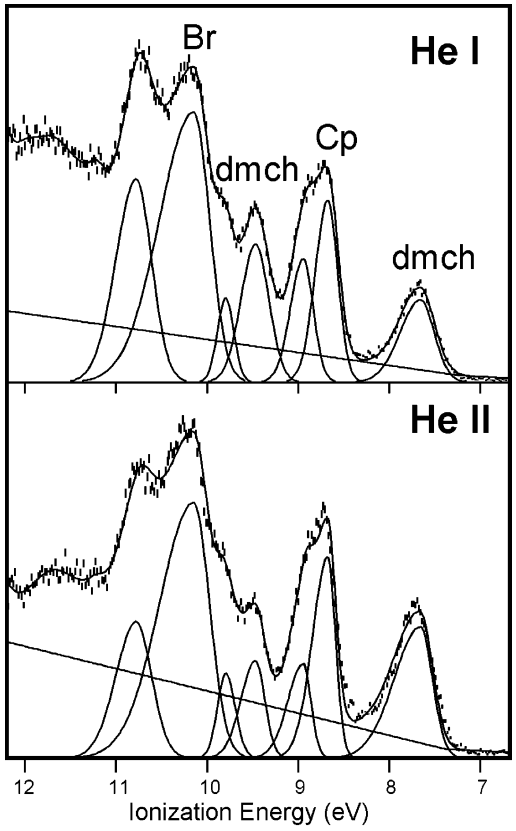

Figure 5. He I and He II photoelectron spectra of Cp(6,6-dmch)$ZrBr_2$.

at 9.80 eV might be due primarily to the second π ionization of 6,6-dmch as supported by He II data, because there is an increase in the intensity of the band at 9.80 eV in the He II spectrum relative to the bands corresponding to chlorine 3p orbitals.

Although individual Cp-based and Cl-based ionizations show some changes in splitting and shifts in energies between Cp_2ZrCl_2 and Cp(6,6-dmch)$ZrCl_2$, it is not evident that there has been any significant change in the charge potential or electron richness at the metal center when 6,6-dmch replaces Cp in these molecules. This contrasts with the situation for lower valent complexes, in which the δ acidities of the pentadienyl ligands exert a large influence.[60−62] Overall, the Cp-based and Cl-based ionizations are in the same general energy positions and the charge potential at the metal appears to be much the same for the two molecules.

Cp(6,6-dmch)$ZrBr_2$. The He I and He II photoelectron spectra of Cp(6,6-dmch)$ZrBr_2$ from 7 to 12 eV are shown in Figure 5. The assignments of the ionization bands are similar to those of Cp(6,6-dmch)$ZrCl_2$. The first ionization at 7.64 eV arises from the pentadienyl ligand, while the next two at 8.65 and 8.91 eV are predominantly Cp π ionizations. Bromine pπ ionizations occur at lower ionization energies (starting from 9.47 eV) than chlorine ionizations, following the electronegativity trend. The intensity of the ionizations in the region from 8 to 10 eV does not increase as dramatically as observed for the Cl case when the photon source is switched from He I to He II, and identification of the second 6,6-dmch ionization in particular is less clear. This observation suggests that there is a greater mixing of Br character with ligand π character in the ionizations, as might be expected from their closer energy proximity.

Cp(6,6-dmch)ZrI_2. The photoelectron spectrum of Cp(6,6-dmch)ZrI_2 reveals that the ionizations from Cp(6,6-dmch)ZrI_2 occur at lower energy compared to Cp(6,6-dmch)$ZrCl_2$ and Cp(6,6-dmch)$ZrBr_2$. The first ionization is similar in appearance to the first ionization of the chloride and bromide complexes and again is assigned to an ionization that is primarily 6,6-dmch in character. Following the first ionization, the spectrum shows four relatively sharp bands in the low-ionization region which are characteristic of iodine-based ionizations. Part of the splitting between the ionizations is the result of spin−orbit coupling in the positive ion states by the heavy iodine. For comparison, the iodine π ionizations of CH_3I are split by 0.62 eV[63] by spin−orbit coupling. Unlike the Cp-based and halogen-based ionizations of Cp(6,6-dmch)$ZrCl_2$ and Cp(6,6-dmch)$ZrBr_2$, these four iodine-based ionizations appear prior to the predominantly Cp π ionizations in the spectrum of Cp(6,6-dmch)ZrI_2. This ordering of ionization bands is verified by He II data, as shown in Figure 6. The relative intensities of the four ionization bands in the region 8.14−9.20 eV decrease compared to the ionization band at 7.58 eV and the bands above 9.20 eV, which supports the assignment of those four bands as originating primarily from iodine.

This pattern is similar to the photoelectron spectrum of Cp_2ZrI_2, which also showed the first iodine pπ ionizations appearing

(60) Ernst, R. D.; Liu, J. Z.; Wilson, D. R. *J. Organomet. Chem.* **1983**, *250*, 257−263.
(61) Newbound, T. D.; Rheingold, A. L.; Ernst, R. D. *Organometallics* **1992**, *11*, 1693−1700.
(62) Gedridge, R. W.; Hutchinson, J. P.; Rheingold, A. L.; Ernst, R. D. *Organometallics* **1993**, *12*, 1553−1558.
(63) Kimura, K.; Katsumata, Y.; Achiba, Y.; Yamazaki, T. *Handbook of He I Photoelectron Spectra of Fundamental Organic Molecules*; Scientific Societies Press: Tokyo, Japan, 1980.

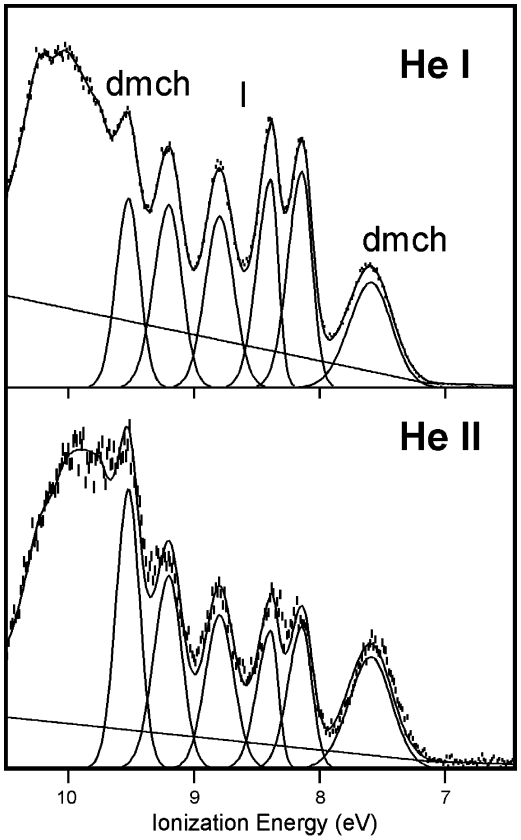

Figure 6. He I and He II photoelectron spectra of Cp(6,6-dmch)ZrI_2.

prior to the cyclopentadienyl π ionizations. Cp_2ZrI_2 is unique among all of these molecules in that it is the only one for which the first ionization is primarily halogen-based. The first iodine pπ ionization of Cp_2ZrI_2 is at 8.13 eV, and the first iodine pπ ionization of Cp(6,6-dmch)ZrI_2 is found here at 8.14 eV. The similarity of these energies indicates that, as for the chlorine-containing molecules discussed earlier, the charge potential at the metal center and throughout the molecule does not change much when 6,6-dmch replaces Cp in these higher valent molecules.

The energy separation between the two 6,6-dmch π ionizations in both Cp(6,6-dmch)$ZrCl_2$ and Cp(6,6-dmch)$ZrBr_2$ is approximately 2 eV. Similarly, the ionization band at 9.52 eV in Cp(6,6-dmch)ZrI_2 is separated 2.07 eV from the first 6,6-dmch π ionization. On the basis of this observation, the band at 9.52 eV is assigned as predominantly the second 6,6-dmch π ionization.

To summarize, the key difference between Cp_2ZrI_2 and Cp(6,6-dmch)ZrI_2 is that in the former the first ionization is predominantly iodine in character whereas in the latter the first ionization is predominantly 6,6-dmch π in character and significantly lower in energy.

Computational Results. The bond lengths and angles calculated using ADF for optimized geometries for the Cp(6,6-dmch)ZrX_2 are presented in Table 2. The calculated Zr−C distances and angles are slightly too long compared to crystallographic data, but they agree well with the basic trends observed for these molecules. Given the substantial lengthening for the Zr−C(1,2,4,5) distances, one can expect that there would be a rather flat potential surface involving these Zr−C(dmch) distances, so that these differences likely represent small energies. The Zr−(6,6-dmch) and Zr−Cp distances calculated for Cp(6,6-dmch)$ZrCl_2$ averaged to be 2.73 and 2.62 Å, respectively, indicating 0.11 Å longer Zr−C bonds for the 6,6-dmch ligand in this Zr(IV) complex. The calculated Zr−C distances to the pentadienyl ligand in Cp(2,6,6-tmch)Zr(PMe_3)$_2$ is 2.55 Å, which is 0.13 Å shorter than the calculated average value of 2.68 Å for the accompanying Cp ligand in this Zr(II) complex. The calculations are thus seen to reproduce reasonably well the observed reversal in dienyl bonding preference.

Orbital surface plots and Kohn−Sham orbital energies for the 10 highest occupied molecular orbitals and the lowest unoccupied molecular orbital of Cp(6,6-dmch)$ZrCl_2$ are shown in Figure 7. Cp(6,6-dmch)$ZrBr_2$ yields very similar results. The computational results agree with the primary features in the experimental photoelectron spectra, with only slight differences occurring in the deeper energy region. Most significantly, the calculations are in agreement with the observation that the first ionization is from an orbital that is predominantly 6,6-dmch in character and is well separated in energy from the second ionization. The first ionization is followed in general by the two Cp-based ionizations and then by predominantly Cl-based π and σ ionizations. The fourth ionization band at 9.80 eV is tentatively assigned to the second 6,6-dmch π ionization on the basis of intensity differences in the He I and He II experiments. The calculation shows that the fourth Kohn−Sham orbital has primarily chlorine pπ character and the fifth has substantial 6,6-dmch character with mixing from the Cp and the Cl's. This difference between experimental and computational results is not very significant when considering the amount of mixing in the molecular orbitals, the approximations in the calculations, the assumptions in relating Kohn−Sham orbital energies to ionization energies, and the closeness of these two orbital energies. The calculated energies of these orbitals are within 0.3 eV and beyond the confidence level for ordering these ionizations by these calculations.

The orbital ordering calculated for Cp(6,6-dmch)ZrI_2 is different from that of Cp(6,6-dmch)$ZrCl_2$ and Cp(6,6-dmch)-$ZrBr_2$ but is in agreement with the experimental assignment. Orbital surface plots for the 10 highest occupied molecular orbitals of Cp(6,6-dmch)ZrI_2 are shown in Figure 8. The highest occupied molecular orbital again is of predominantly 6,6-dmch π character with some halogen character. The four iodine pπ orbitals and Zr−I σ orbitals appear prior to the Cp π orbitals in Cp(6,6-dmch)ZrI_2, unlike the halogen-based orbitals of both Cp-(6,6-dmch)$ZrCl_2$ and Cp(6,6-dmch)$ZrBr_2$. There is also less mixing with the Cp and 6,6-dmch π orbitals, which occur at higher energies and are depicted by orbitals HOMO−7 through HOMO−9. The second 6,6-dmch π orbital in the calculation appears at higher energy (more stable) than those of the Zr−I σ and Cp π orbitals. However, the experimental observations suggest that the second 6,6-dmch π ionization appears prior to the Cp π and Zr−I σ ionizations, and it is separated by ca. 2 eV from the first 6,6-dmch π ionization.

Time-dependent density functional theory provides a basic method for the calculation of excitation energies and many related response properties on different chemical systems.[64−66]

(64) van Gisbergen, S. J. A.; Baerends, E. J.; Rosa, A.; Ricciardi, G. *J. Chem. Phys.* **1999**, *111*, 2499−2506.
(65) Jamorski, C.; Casida, M. E.; Salahub, D. R. *J. Chem. Phys.* **1996**, *104*, 5134−5147.
(66) van Gisbergen, S. J. A.; Snijders, J. G.; Baerends, E. J. *J. Chem. Phys.* **1995**, *103*, 9347−9354.

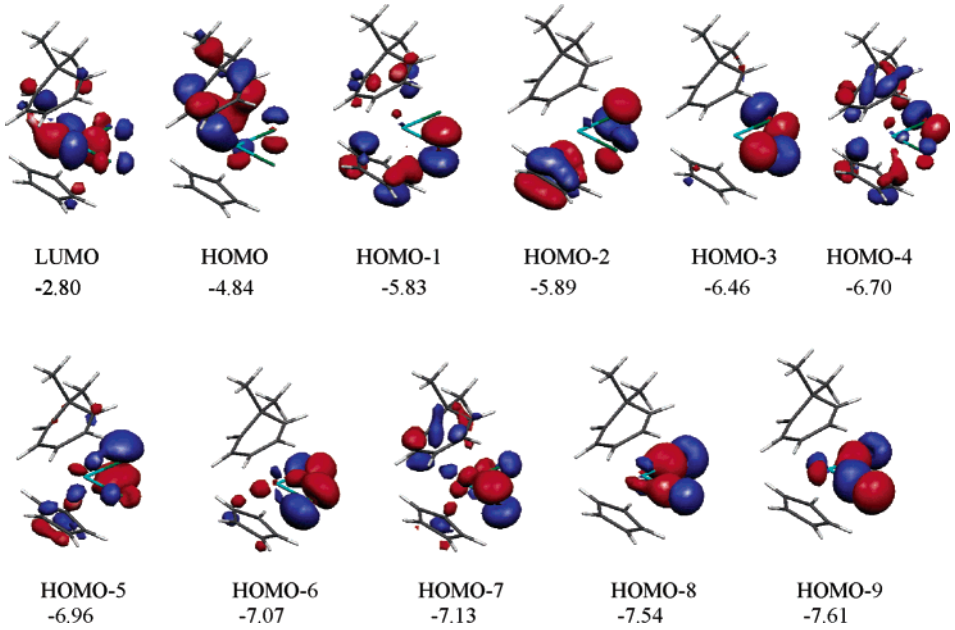

Figure 7. Orbital surfaces (value = ±0.05) and energies (eV) for frontier orbitals of Cp(6,6-dmch)$ZrCl_2$.

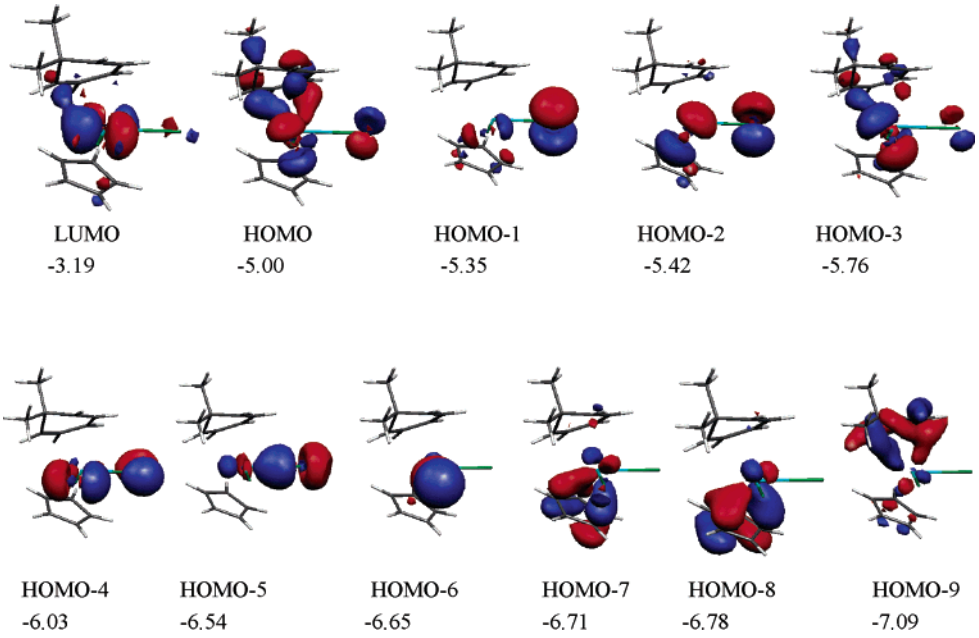

Figure 8. Orbital surfaces (value = ±0.05) and energies (eV) for frontier orbitals of Cp(6,6-dmch)ZrI_2.

Table 5. HOMO−LUMO Separation (from DFT), Dipole-Allowed Singlet Excitation Energies (from TD-DFT), and Experimental Excitation Energies for the HOMO−LUMO Transition Except for Cp_2ZrI_2 [a]

molecule	HOMO–LUMO separation (eV)	excitation energy (eV) calc	excitation energy (eV) [expt]	oscillator strength ($\times 10^{-2}$)	primary character
Cp_2ZrCl_2	2.92	3.15	[3.62]	0.59	Cp → Zr
Cp_2ZrBr_2	2.63	2.83	[3.31]	0.33	Cp → Zr
Cp_2ZrI_2	2.22	2.68[b]	[3.08]	6.00	I → Zr
Cp(6,6-dmch)$ZrCl_2$	2.04	2.34	[2.82]	0.80	dmch → Zr
Cp(6,6-dmch)$ZrBr_2$	1.95	2.23	[2.67]	0.69	dmch → Zr
Cp(6,6-dmch)ZrI_2	1.82	2.06	[2.54]	0.90	dmch → Zr

[a] See text for explanation.

Calculations using TD-DFT on both Cp_2ZrX_2 and Cp(6,6-dmch)ZrX_2 (X = Cl, Br, I) molecules were performed in order to compare the trends in excitation energies. The calculated and experimental excitation energies and the primary character for the HOMO−LUMO transition are given in Table 5. The HOMO is primarily Cp in character for Cp_2ZrCl_2 and Cp_2ZrBr_2, and it is primarily 6,6-dmch in character for the Cp(6,6-dmch)ZrX_2 molecules. The Cp_2ZrI_2 molecule is unique in this set in that the HOMO is iodine in character and the HOMO−LUMO transition has very low oscillator strength. The observed

excitation energy reported for Cp_2ZrI_2 likely involves the HOMO−2 to LUMO transition, instead of HOMO to LUMO, because the HOMO−2 to LUMO transition is the first that has appreciable oscillator strength. The lowering of excitation energy upon changing the halogen from Cl to Br to I is observed for both types of systems. The calculated excitation energies of the Cp(6,6-dmch)ZrX_2 molecules are all seen to be substantially lower than any of those obtained for the Cp_2ZrX_2 molecules, directly leading to the intense colors of the pentadienyl species compared to the Cp_2ZrX_2 molecules. These are the same trends observed in the experimental excitation energies of the Cp_2ZrX_2 and Cp(6,6-dmch)ZrX_2 molecules. The calculated excitation energies are all about half an electronvolt lower than the experimental measures from the absorption spectra.

Discussion

The synthesis of a general series of stable high-valent metal pentadienyl complexes represents the achievement of a long sought goal in this area, given the extreme favorability for pentadienyl ligands to bond to metals in low oxidation states. The electropositive nature, large size, and great favorability of the tetravalent state may all contribute to the stability of this general class of Zr compounds. Indeed, while a few isolated examples of higher oxidation state complexes have been reported,[24,67−71] the presence of strong π donor ligands seems to have been a key to their stability, although complexes with the larger, more ionic U(IV) center are known.[72] The Cp(6,6-dmch)ZrX_2 series of complexes actually allows us to gain some understanding of the structural and bonding differences between the pentadienyl Zr(IV) and Zr(II) species and, importantly, for the first time provides for a direct comparison of the bonding of the two dienyl ligand types, pentadienyl and cyclopentadienyl, in high oxidation state species.

X-ray diffraction data reveal that, as in the other recently reported Zr(IV) pentadienyl complexes,[5,6,23,24] each of these species possesses a particularly short Zr−C3 distance (Table 2), which, together with the expected differences in C−C bond lengths, reflects a significant contribution from the resonance hybrid shown below.

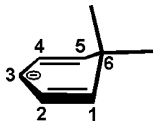

The substantial interaction with C3 in these Zr(IV) complexes is consistent with early MO studies that revealed substantial localization of negative charge on this position[73,74] and also with the structural result of a highly ionic Nd(III) pentadienyl complex, for which the Nd−C3 bonds were also the shortest.[75] The ADF calculations performed in this study agree that the Zr−C3 distance is shorter than the other Zr−C distances and that the negative charge on C3 is greater than on the other carbons, although the difference of about 0.02 electron in charge is relatively small.[76,77]

The Zr−C distances for the 6,6-dmch ligand in these Zr(IV) complexes are 0.1 Å longer on average than the Zr−C distances to the Cp ligand (Table 2). The opposite trend is observed for similar Zr(II) complexes, as well as for Ti(II),[4−6,78] V(II),[60−62] and even Cr(II)[79,80] analogues. The calculations reproduce this trend. Although the asymmetry of the Zr−C(6,6-dmch) distances distorts the comparison somewhat, the fact that in the Zr(IV) complex not even the (short) Zr−C3 distance is 0.1 Å shorter than any of those for the Cp ligand carbon atoms clearly demonstrates a remarkable reversal in the relative favorability of the Zr−(dienyl) bonding.

The very clear preference for pentadienyl ligands to bond to transition metals in low ($\leq +2$) oxidation states has long been evident[3] and may be traced both to the low orbital overlap that would be expected between the wide pentadienyl ligand and the rather contracted orbitals of the higher valent metal center and to the high δ acidities of pentadienyl ligands. The latter factor can be attributed in part to the lower energy of one of the pentadienyl π^* molecular orbitals, but may also derive from the wide geometric nature of the pentadienyl ligand, which leads to a M−ligand plane separation that can be 0.5 Å or more shorter than that for the Cp ligand. Naturally, the fact that this Zr(IV) complex has a d^0 configuration would also preclude δ back-bonding, in accord with the MO results.

The molecular orbital surface picture (value = $\pm$0.05) for the HOMO of CpZr(2,6,6-tmch)$(PMe_3)_2$ seen below shows a prominent δ bonding interaction between the pentadienyl fragment and Zr center, in which the occupied, predominantly metal d orbital of the formally Zr(II) metal center back-bonds to the low-lying empty pπ orbital of the pentadienyl ligand. Such an interaction between Cp and the metal is much less significant and not visible in the orbital plot. As noted above, the high δ acidities of pentadienyl ligands as opposed to cyclopentadienyl ligands play a large role in the reversal in bond length comparisons between the metal and 6,6-dmch and Cp ligands in these Zr(II) and Zr(IV) molecules.

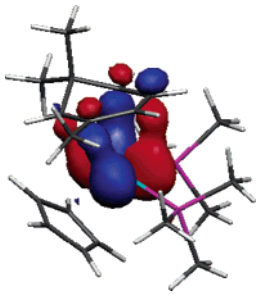

(67) Lentz, M. R.; Fanwick, P. E.; Rothwell, I. P. *Organometallics* **2003**, *22*, 2259−2266.
(68) Feng, S.; Klosin, J.; Kruper, W. J., Jr.; McAdon, M. H.; Neithamer, D. R.; Nickias, P. N.; Patton, J. T.; Wilson, D. R.; Abboud, K. A.; Stern, C. L. *Organometallics* **1999**, *18*, 1159−1167.
(69) Gutierrez, A.; Wilkinson, G.; Hussainbates, B.; Hursthouse, M. B. *Polyhedron* **1990**, *9*, 2081−2096.
(70) Gavenonis, J.; Tilley, T. D. *J. Am. Chem. Soc.* **2002**, *124*, 8536−8537.
(71) Gavenonis, J.; Tilley, T. D. *Organometallics* **2002**, *21*, 5549−5563.
(72) Baudry, D.; Bulot, E.; Charpin, P.; Ephritikhine, M.; Lance, M.; Nierlich, M.; Vigner, J. *J. Organomet. Chem.* **1989**, *371*, 163−174.
(73) Bates, R. B.; Gosselin, D. W.; Kaczynski, J. A. *Tetrahedron Lett.* **1967**, 199−204.
(74) Brickstock, A.; Pople, J. A. *Trans. Faraday Soc.* **1954**, *50*, 901−911.
(75) Ernst, R. D.; Cymbaluk, T. H. *Organometallics* **1982**, *1*, 708−713.
(76) te Velde, G. *Numerical Integration and Other Methodological Aspects of Bandstructure Calculations, in Chemistry*; Vrije Universiteit: Amsterdam, 1990.
(77) Bickelhaupt, F. M.; van Eikema Hommes, N. J. R.; Fonseca Guerra, C.; Baerends, E. J. *Organometallics* **1996**, *15*, 2923−2931.
(78) Melendez, E.; Arif, A. M.; Ziegler, M. L.; Ernst, R. D. *Angew. Chem., Int. Ed. Engl.* **1988**, *27*, 1099−1101.
(79) Freeman, J.; Hallinan, N. C.; Arif, A. M.; Gedridge, R. W.; Ernst, R. D.; Basolo, F. *J. Am. Chem. Soc.* **1991**, *113*, 6509−6520.
(80) Bovino, S. C.; Coates, G.; Banovetz, J.; Waymouth, R.; Straus, D. A.; Ziller, J. *Inorg. Chim. Acta* **1993**, *203*, 179−183.

Table 6. Experimental and Calculated First Ionization Energies[a] and (Primary Character)

	Cp_2ZrX_2		$Cp(6,6\text{-dmch})ZrX_2$	
X	expt	calc	expt	calc
Cl	8.62 (Cp)	8.03	7.63 (6,6-dmch)	7.17
Br	8.53 (Cp)	7.85	7.66 (6,6-dmch)	7.13
I	8.13 (I)	7.61	7.59 (6,6-dmch)	7.07

[a] All energies in eV.

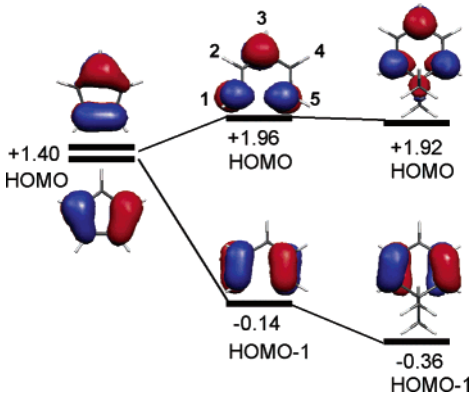

Figure 9. Correlation between molecular orbital energies (eV) of Cp^-, "open Cp^-" (at C_1 to C_5 coordinates of 6,6-$dmch^-$), and 6,6-$dmch^-$ ligands.

The photoelectron spectra of $Cp(6,6\text{-dmch})ZrX_2$ complexes (for which X = Cl, Br, I) reveal interesting features in their electronic structure in comparison to the more familiar Cp_2ZrX_2 molecules. The first ionization energies and characters of these molecules are compared in Table 6. The first ionization is predominantly 6,6-dmch π in character in all three 6,6-dmch-containing molecules regardless of the halogen and is considerably lower in energy than the first ionization of the bis-Cp molecules. In the bis-Cp series of molecules, the first ionization is predominantly Cp in character for the chloride and bromide molecules but changes to predominantly halogen character for the iodide. The experimental first ionization energies are similar for the chloride and bromide molecules in the bis-Cp series, but the first ionization energy of the iodide molecule is much less due to the change of the first ionization to predominantly halogen character. In contrast, all three dmch-containing molecules have approximately the same first ionization energies regardless of the halogen because the HOMO remains 6,6-dmch-based. These are the same basic trends observed in the calculated first ionization energies for both Cp_2ZrX_2 and $Cp(6,6\text{-dmch})ZrX_2$ molecules, although the calculated first ionization energies underestimate the experimental values by about half an electronvolt.

Figure 9 illustrates why the ionization due to the 6,6-dmch ring appears at lower ionization energy than that of the Cp ring. On the left of Figure 9 are the orbitals and energies of the degenerate e_1'' orbitals of the cyclopentadienyl anion calculated by density functional theory. The middle of Figure 9 shows the orbitals and energies that result when the carbon and hydrogen atoms of the cyclopentadienyl ring are moved to the locations of the corresponding atoms of 6,6-dmch. The low ionization energy of the 6,6-dmch HOMO follows from the increased C1···C5 separation in 6,6-dmch compared to Cp. In Cp one of the degenerate π orbitals is bonding between C1 and C5 and the other is antibonding. Increasing the C1···C5 distance decreases the bonding stabilization in the first orbital and decreases the antibonding destabilization in the second. Adding the bridging carbon atom with its two methyl groups to the pentadienyl to complete the structure of the 6,6-dmch ligand only slightly perturbs the orbitals and their energies, as shown on the right of Figure 9.

The LUMO of these molecules is primarily metal in character, lying in the plane of the metal−halogen bonds as shown in Figures 7 and 8. It corresponds to the lower a_1 type metal-based orbital of bent metallocenes described by Hoffmann.[81] It has the correct symmetry to interact with the in-plane pπ orbitals of the halogens. The orbital energy of the LUMO changes very little with a change in halogen from Cl to Br to I, and most importantly, the substitution of 6,6-dmch in place of Cp has a small effect on the energy of the LUMO (less than 0.1 eV according to the calculations). This small shift in the LUMO energy is consistent with the observation from the photoelectron spectra that there is very little change in the charge potential at the metal when 6,6-dmch replaces Cp in these molecules.

The intense colors of these molecules compared to the bis-(cyclopentadienyl)zirconium analogues follows from the trends in the HOMO−LUMO gap. Table 5 lists the calculated HOMO−LUMO gaps for the $Cp(6,6\text{-dmch})ZrX_2$ and Cp_2ZrX_2 molecules. As these are d^0 molecules, the origin of color is most likely due to ligand-to-metal charge-transfer bands. All three $Cp(6,6\text{-dmch})ZrX_2$ molecules have approximately 2 eV HOMO−LUMO separations, resulting in absorption in the visible region. On the other hand, the Cp_2ZrX_2 molecules have a larger HOMO−LUMO separation of about 3 eV, which corresponds to the absorption in the near-UV region. The reason for the smaller HOMO−LUMO gap in the molecules containing 6,6-dmch follows directly from the lower ionization energy of the 6,6-dmch-based HOMO, while the metal-based LUMO remains essentially unchanged.

Previous studies on the open pentadienyl complex $Fe(\eta^5\text{-}C_5H_7)_2$ and ferrocene also show that $Fe(\eta^5\text{-}C_5H_7)_2$ has a smaller HOMO−LUMO gap compared to ferrocene.[56,82] In this case, the first ionization is metal-based for each molecule, and the LUMO is ligand-based, but the reason for the smaller gap is similar. The increase in the C1···C5 distance from Cp to pentadienyl splits the degenerate virtual e_2'' orbitals of Cp to create a pentadienyl-based LUMO that is lower in energy. The stabilization of the pentadienyl-based LUMO contributes to the smaller HOMO−LUMO gap and the δ acidity of the pentadienyl ligand.

Conclusions

The isolation of the $Cp(6,6\text{-dmch})ZrX_2$ complexes has allowed for the first direct comparisons to be made between metal−pentadienyl and metal−Cp bonding for a high oxidation state metal center. The experimental results together with calculations presented here show that there is a marked reversal in the relative bonding capabilities of cyclopentadienyl and open pentadienyl ligands as compared to the lower valent analogues. This reversal can readily be explained by a loss in δ bonding and metal−pentadienyl overlap for higher oxidation state metal centers. The substantial δ back-bonding ability of the pentadienyl ligands as compared to Cp has been confirmed through the calculations and spectroscopic data.

(81) Lauher, J. W.; Hoffmann, R. *J. Am. Chem. Soc.* **1976**, *98*, 1729−1742.
(82) Ernst, R. D. *Chem. Rev.* **1988**, *88*, 1255−1291.
(83) Yeh, J. J.; Lindau, I. *Atom. Data Nucl. Data* **1985**, *32*, 1.

The gas-phase photoelectron spectroscopic studies reveal that the highest occupied molecular orbital for the Cp(6,6-dmch)-ZrX_2 molecules is primarily 6,6-dmch in character, which leads to a significantly lower ionization energy for these molecules compared to the Cp-only analogues. In corresponding Cp(6,6-dmch)ZrX_2 and Cp_2ZrX_2 molecules, the charge potential at the metal and the energy of the metal-based lowest unoccupied molecular orbital remain essentially unchanged, resulting in a smaller HOMO−LUMO separation, which gives an intense color to the Cp(6,6-dmch)ZrX_2 molecules.

These altered electronic features can be expected to enhance the reactivity properties observed for higher valent metal−pentadienyl molecules, as has already been found for lower valent species. The access to the first pentadienyl analogues of the ubiquitous Cp_2MX_2 complexes also offers an opportunity to explore an entirely new flavor of metal−pentadienyl chemistry, not just for zirconium, but in all likelihood for other early second- and third-row transition metals as well. Already it is clear that the reactivities of these complexes differ dramatically from that of the more normal, lower valent species.[28]

Acknowledgment. D.L.L. thanks the U.S. Department of Energy and the National Science Foundation (CHE-0078457) for support. R.D.E. thanks the Petroleum Research Fund, Research Corporation, and the University of Utah for support.

Supporting Information Available: CIF files for each of the crystal structures included. This material is available free of charge via the Internet at http://pubs.acs.org.

JA040123+